Naval Research Laboratory

Washington, DC 20375-5320

NRL/MR/6930--18-9806

Colorimetric Environmental Sensor: Aqueous Indicator Screening (Part 1)

Brandy J. White
Martin H. Moore

Laboratory for the Study of Molecular Interfacial Interactions
Center for Bio/Molecular Science & Engineering

Kaleb Franco

Forest Park High School
Woodbridge, VA

Anthony P. Malanoski

Laboratory for Biosensors and Biomaterials
Center for Bio/Molecular Science & Engineering

September 17, 2018

REPORT DOCUMENTATION PAGE

Form Approved
OMB No. 0704-0188

1. REPORT DATE *(DD-MM-YYYY)*
17-09-2018

2. REPORT TYPE
Memorandum Report

3. DATES COVERED *(From - To)*
9/30/2013-08/01/2018

4. TITLE AND SUBTITLE

Colorimetric Environmental Sensor: Aqueous Indicator Screening (Part I)

5a. CONTRACT NUMBER

5b. GRANT NUMBER

5c. PROGRAM ELEMENT NUMBER

6. AUTHOR(S)

Brandy J. White, Martin H. Moore, Kaleb Franco* and Anthony P. Malanoski

5d. PROJECT NUMBER

5e. TASK NUMBER

5f. WORK UNIT NUMBER
69-6594

7. PERFORMING ORGANIZATION NAME(S) AND ADDRESS(ES)

Center for Bio/Molecular Science & Engineering
Naval Research Laboratory
4555 Overlook Avenue, SW
Washington, DC 20375-5344

8. PERFORMING ORGANIZATION REPORT NUMBER

NRL/MR/6930--18-9806

9. SPONSORING / MONITORING AGENCY NAME(S) AND ADDRESS(ES)

10. SPONSOR / MONITOR'S ACRONYM(S)

NRL 6.2

11. SPONSOR / MONITOR'S REPORT NUMBER(S)

12. DISTRIBUTION / AVAILABILITY STATEMENT

DISTRIBUTION STATEMENT A: Approved for public release; distribution is unlimited.

13. SUPPLEMENTARY NOTES
*KF SEAP: Forest Park High School, Woodbridge, VA

14. ABSTRACT

This report is work focused on a component of an effort intended to develop wireless sensor networks for real-time monitoring of airborne targets across a broad area. The performance of the sensor devices will depend heavily on the selection of appropriate indicator elements in design of the arrays. This document summarizes results for aqueous screening of meso-tetra(4-aminophenyl) porphyrin (N4TPP) and metalloporphyrin (XN4TPP) variants of this structure.

15. SUBJECT TERMS

environmental sensor, chemical sensor, colorimetric, porphyrin

16. SECURITY CLASSIFICATION OF:			**17. LIMITATION OF ABSTRACT**	**18. NUMBER OF PAGES**	**19a. NAME OF RESPONSIBLE PERSON**
					Brandy J. White
a. REPORT	**b. ABSTRACT**	**c. THIS PAGE**	Unclassified Unlimited	27	**19b. TELEPHONE NUMBER** *(include area code)*
Unclassified Unlimited	Unclassified Unlimited	Unclassified Unlimited			(202) 404-6100

Standard Form 298 (Rev. 8-98)
Prescribed by ANSI Std. Z39.18

This page intentionally left blank.

CONTENTS

FIGURES

TABLES

EXECUTIVE SUMMARY

In October 2012, the Center for Bio/Molecular Science and Engineering at the Naval Research Laboratory (NRL) began an effort intended to develop wireless sensor networks for real-time monitoring of airborne targets across a broad area. The goal was to apply the spectrophotometric characteristics of porphyrins and metalloporphyrins in a colorimetric array for detection and discrimination of changes in the chemical composition of environmental air samples. The performance of the device will depend heavily on the selection of appropriate indicator elements in design of the arrays. The current document summarizes results for aqueous screening of meso-tetra(4-aminophenyl) porphyrin (N_4TPP) and metalloporphyrin (XN_4TPP) variants of this structure.

This page intentionally left blank.

COLORIMETRIC ENVIRONMENTAL SENSOR: AQUEOUS INDICATOR SCREENING

INTRODUCTION

In October 2012, the Center for Bio/Molecular Science and Engineering at the Naval Research Laboratory (NRL) began an effort (69-6594) intended to develop wireless sensor networks for real-time monitoring of airborne targets across a broad area. The goal was to apply the spectrophotometric characteristics of porphyrins and metalloporphyrins in a colorimetric array for detection and discrimination of changes in the chemical composition of environmental air samples. The effort encompasses hardware, software, and firmware development as well as development of algorithms for identification of event occurrence and discrimination of targets. [1, 2, 3, 4] The performance of these components is dependent on selection of the appropriate indicator elements in design of the array. The current document summarizes results for liquid screening of meso-tetra(4-aminophenyl) porphyrin (N_4TPP) and metalloporphyrin (XN_4TPP) variants of this structure (Figure 1).

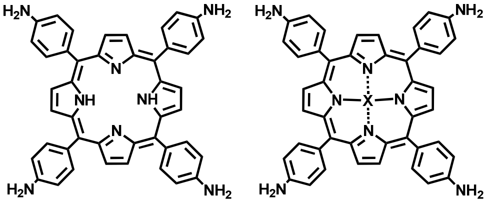

Fig. 1 — Molecular structures of meso-tetra(4-aminophenyl) porphyrin (N_4TPP) and the metalloporphyrin (XN_4TPP) variants of this structure.

The targets utilized in the evaluation of these indicator materials are ethanol, methanol, and isopropanol. These targets were selected for prototype development because they present a low degree of hazard allowing for their use in a range of environments and scenarios while providing the potential for evaluation of the full sensor package. The screening approach uses aqueous solutions of the porphyrins to which varying concentrations of the alcohols are added. The changes in absorbance allow for calculation of affinity coefficients. The expectation is that the affinity coefficient between the target and indicator will be related to the sensitivity of the paper supported indicator for that target.

METHODS

Meso-tetra(4-aminophenyl) porphyrin (N_4TPP) was obtained from Frontier Scientific (Logan, UT). Metalloporphyrin variants of N_4TPP were prepared by reflux. [1, 2, 3] The porphyrin (20 mg) was dissolved in 2 mL water with hydrochloric acid (sufficient only to dissolve the porphyrin full). The metal salt was added to this solution in a 3:1 molar ratio with the porphyrin. The total volume was brought to 100 mL with deionized water and refluxed overnight. The volume of the resulting solution was reduced to 20 mL through rotary evaporation. Prepared metal salt solutions were stored in the dark at room temperature. The metal salts used here were: yttrium (III) chloride, iron (II) sulfate, nickel (II) chloride, zinc chloride, copper (II) chloride, cadmium chloride, cerium (III) chloride, silver chloride, and cobalt (II) chloride.

Manuscript approved September 17, 2018.

Absorbance spectra of the porphyrin solutions were collected using an Agilent 8453 UV/vis spectrophotometer (Agilent Technologies, Inc., Santa Clara, CA) from 190 to 1100 nm at 2 nm resolution. Solutions were prepared in a quartz cuvette using deionized water (18.2 MΩ; 3 mL) and 10 μL of the prepared porphyrin solution (2 mg/mL, above). The absorbance spectrum of this as prepared solution was compared to that of the same solution amended with ethanol, methanol, or isopropanol added in 10 μL aliquots. Final concentrations are indicated in the text and figure captions.

RESULTS

A series of metalloporphyrin variants were prepared based on the N$_4$TPP structure. Absorbance spectra of these variants were collected in aqueous solution (Figure 2). The absorbance of the porphyrin (or metalloporphyrin) in aqueous solution was used as a point of comparison for the absorbance spectra of the same solution amended with ethanol, methanol, or isopropanol (Figure 3). Ethanol concentrations were increased through sequential addition of 10 μL aliquots for final concentrations of 57, 113, 169, 225, 280, 335, 390, and 444 mM. The same series were collected for isopropanol with final concentrations of 43, 86, 129, 171, 214, 256, 298, and 339 mM and for methanol with final concentrations of 82, 163, 244, 325, 404, 483, 563, and 641 mM (Figure 3; full data set provided in Appendix A). The porphyrin concentration was 9.86 μM in the initial solution. Absorbance spectra have been corrected for dilution resulting from target addition. Difference spectra were calculated as the point by point subtraction of the porphyrin + alcohol solution minus the porphyrin solution alone (Figure 3).

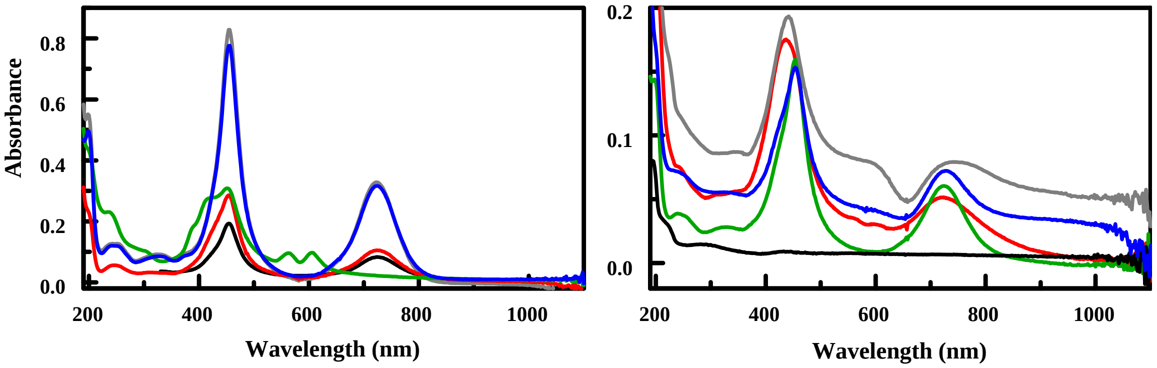

Fig. 2 — Absorbance spectra of the porphyrin and metalloporphyrin variants considered (9.86 μM in water): (left) N$_4$TPP (black), CeN$_4$TPP (red), CuN$_4$TPP (green), NiN$_4$TPP (blue), YN$_4$TPP (gray); (right) AgN$_4$TPP (red), CdN$_4$TPP (green), CoN$_4$TPP (gray), FeN$_4$TPP (black), ZnN$_4$TPP (blue).

The difference spectra (Figure 3) were used to identify peak and trough positions for additional analysis. The change in absorbance for the characteristic peak / trough positions were plotted versus target concentration (Figure 4). Fitting parameters were determined based on an expression that combines the standard form of a binding interaction and the Beer-Lambert Law. This approach assumes: (1) the porphyrin-analyte complex is 1:1; [5] (2) Beer's Law is followed by the porphyrin, analyte, and the porphyrin-analyte complex; and (3) the extinction coefficients of the free reagents at the wavelength under consideration are significantly different from that of the porphyrin-analyte complex. The resulting expression provides the relationship between the absorbance change (ΔA) and the variables porphyrin concentration ([P]), analyte concentration ([L]), and complex stability constant (K_{11}). [6]

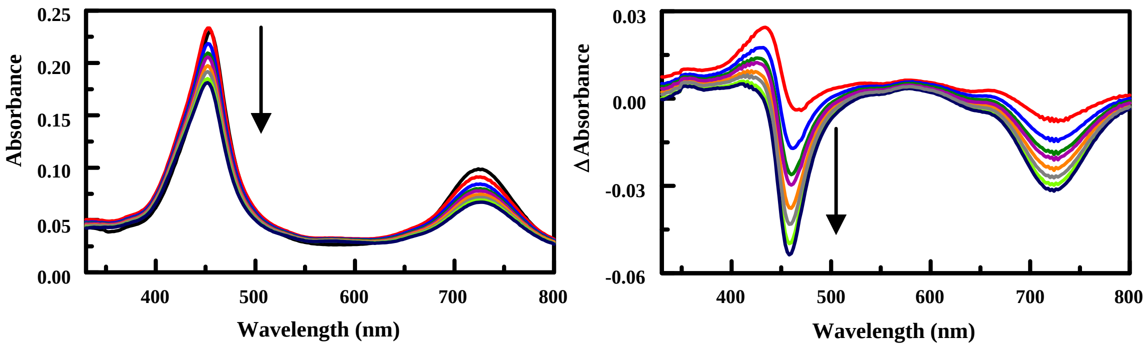

Fig. 3 — Absorbance spectra of N_4TPP (9.86 µM; left) in the absence and presence of increasing concentrations of isopropanol: 43, 86, 129, 171, 214, 256, 298, and 339 mM. Arrows indicate increasing target concentration. Absorbance spectra have been corrected for dilution resulting from target addition. Difference absorbance spectra (right) are calculated as porphyrin + target minus porphyrin.

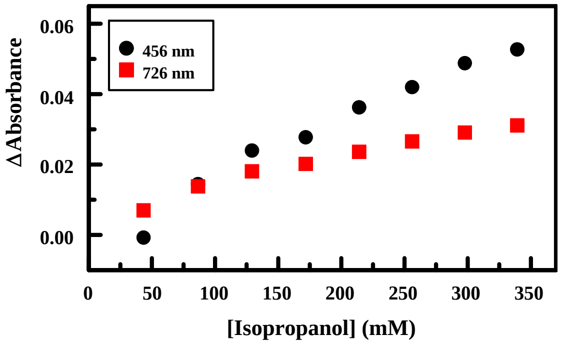

Fig. 4 — The concentration dependence of features in the absorbance spectra is presented. Here, the change in absorbance at the trough positions 456 (black) and 726 nm (red) is plotted against target concentration.

Derivation of the final expression begins with the Beer-Lambert Law stating:

$$A_0 = \varepsilon_P b[P_t]$$

where A_0 is the initial absorbance of the porphyrin, $[P_t]$ is the total porphyrin concentration, ε_P is the extinction coefficient at the wavelength under consideration, and b is the path length for the measurement. In the presence of analyte (total concentration $[L_t]$), the absorbance of a solution containing the same total porphyrin concentration is:

$$A_L = \varepsilon_P b[P] + \varepsilon_L b[L] + \varepsilon_{11} b[PL].$$

Here, ε_L and ε_{11} are the extinction coefficients of the analyte and the complex, respectively, and $[PL]$ is the concentration of the complex. If the reference spectrum is taken against a ligand spectrum at $[L_t]$ or the ligand does not absorb in the considered region, this expression becomes:

$$A_L = \varepsilon_P b[P] + \varepsilon_{11} b[PL]\ .$$

The change in absorbance upon addition of ligand is then:

$$\Delta A = \varepsilon_P b[P] + \varepsilon_{11} b[PL] - \varepsilon_P b P_t$$

Recalling that $P_t = [P] + [PL]$ and defining $\Delta\varepsilon_{11} = \varepsilon_{11} - \varepsilon_p$, the expression can be rewritten:

$$\Delta A = \Delta\varepsilon_{11} b[PL]$$

The standard binding isotherm is of the form:

$$[PL] = \frac{[P_t]K[L]}{1 + K[L]}$$

yielding a final expression of:

$$\Delta A = \Delta\varepsilon_{11} b \frac{[P_t]K[L]}{1 + K[L]}$$

Here, $[L_t] >> [P_t]$, so we can approximate $[L] = [L_t]$.

Fitting parameters for the data sets are provided in Table 1. Fits were based on two wavelengths identified based on the prominent features in the difference spectra. The determined difference extinction coefficients varied across three orders of magnitude with the iron metal complex yielding the lowest values and the copper and porphyrin alone variants yielding the largest values. Extinction coefficients may have some impact on the performance of indicator materials in the final devices; however, some of this difference may be corrected through increasing the porphyrin loading in the supported indicator system. In addition, the prototype devices use the full spectrum of reflected light, rather than absorbance at a single wavelength. The affinity coefficients are expected to provide a more valuable point of comparison; these are summarized in Figure 5. If all extinction coefficients were equal, a larger affinity coefficient would provide a larger change in absorbance for a given indicator and target concentration.

Table 1 – Fit Parameters for the Porphyrin Indicators

Porphyrin	**Target**	**K (mM^{-1})**	**Wavelength (nm)**	**$\Delta\varepsilon_{11}$ (mM^{-1}·cm^{-1})**	**Wavelength (nm)**	**$\Delta\varepsilon_{11}$ (mM^{-1}·cm^{-1})**
N_4TPP	Ethanol	5.29E-3	456	15.74	730	6.77
	Isopropanol	7.68E-4	456	25.71	726	16.54
	Methanol	1.38E-3	460	8.15	724	6.87
AgN_4TPP	Ethanol	9.82E-3	458	7.89	726	3.16
	Isopropanol	4.50E-3	453	7.35	402	2.46
	Methanol	8.19E-3	458	3.75	713	1.71
CdN_4TPP	Ethanol	3.95E-3	456	10.45	726	4.25
	Isopropanol	2.05E-2	458	4.44	582	1.33
	Methanol	4.33E-3	434	3.07	714	0.93
CeN_4TPP	Ethanol	1.16E-2	466	11.05	728	5.60
	Isopropanol	2.79E-2	454	10.12	275	0.84
	Methanol	6.99E-3	456	9.69	730	4.15
CoN_4TPP	Ethanol	6.69E-3	442	5.05	578	2.43
	Isopropanol	--	442	--	570	--
	Methanol	5.51E-3	456	2.34	730	1.50
CuN_4TPP	Ethanol	2.38E-3	412	11.01	452	8.07
	Isopropanol	2.91E-3	416	9.46	454	11.29
	Methanol	2.24E-4	412	27.31	452	21.01
FeN_4TPP	Ethanol	6.43e-3	456	0.74	720	0.29
	Isopropanol	--	454	--	730	--
	Methanol	1.95E-2	454	0.60	730	0.23
NiN_4TPP	Ethanol	2.51E-3	456	32.89	720	13.27
	Isopropanol	6.77E-3	454	23.87	730	9.68
	Methanol	3.89E-3	456	12.57	720	4.93
YN_4TPP	Ethanol	2.28E-3	456	16.55	720	6.12
	Isopropanol	1.71E-3	458	14.35	720	4.75
	Methanol	1.40E-3	456	13.18	720	4.42
ZnN_4TPP	Ethanol	1.50E-2	456	5.03	730	2.23
	Isopropanol	5.38E-3	458	6.75	720	3.10
	Methanol	2.78E-3	456	5.24	720	1.73

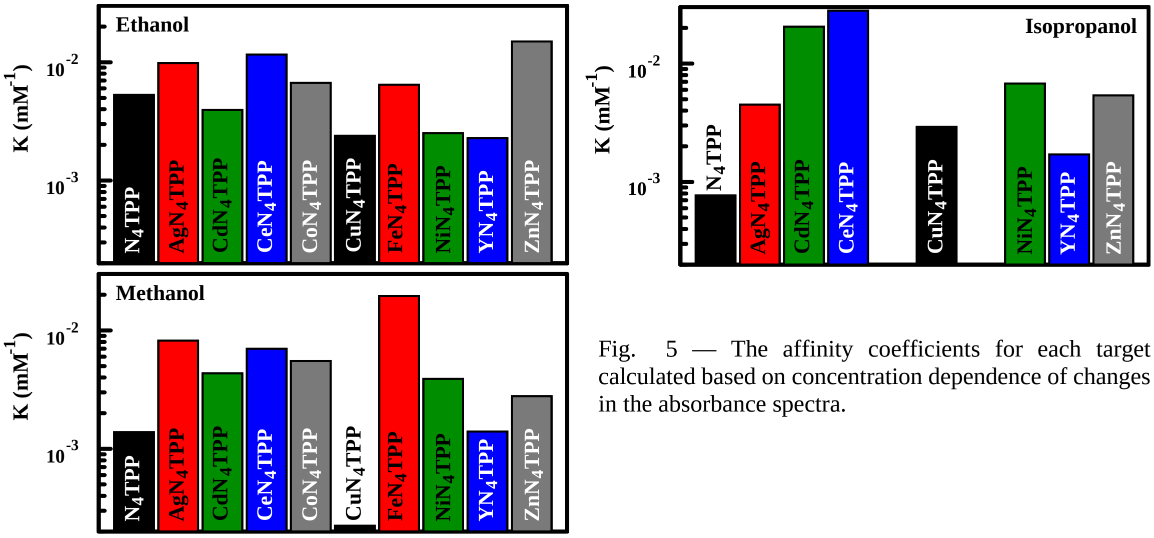

Fig. 5 — The affinity coefficients for each target calculated based on concentration dependence of changes in the absorbance spectra.

CONCLUSIONS

The data provided here is an initial study intended to support development of indicator arrays for use in the NRL prototype environmental sensor system. The meso-tetra(4-aminophenyl) porphyrin (N_4TPP) variants are sensitive to the alcohol model targets. Exceptions include the copper variant of this porphyrin, which shows little response to methanol, and the cobalt and iron porphyrins, which are not sensitive to isopropanol. The ongoing effort will screen additional porphyrin structures, including meso-tetra(4-sulfonatophenyl) porphyrin (S_4TPP) and meso-tetra(4-carboxyphenyl) porphyrin (C_4TPP). Additional work will also provide data on screening of the paper supported versions of these indicators. The overall goal is to design an array of elements that provide the potential for discrimination of targets based on the relative response of the individual elements.

ACKNOWLEDGEMENTS

K. Franco was at NRL during the summer of 2018 through the Office of Naval Research (ONR) Science & Engineering Apprenticeship Program (SEAP).

REFERENCES

1. B.J. Johnson; J.S. Erickson; J. Kim; A.P. Malanoski; I.A. Leska; S.M. Monk; D.J. Edwards; T.N. Young; J. Verbarg; C. Bovais; R.D. Russell; D.A. Stenger, "Miniaturized reflectance devices for chemical sensing," *Meas. Sci. Technol.* **25**, 095101 (2014).
2. B.J. Johnson; R. Liu; R.C. Neblett; A.P. Malanoski; M. Xu; J.S. Erickson; L. Zang; D.A. Stenger; M.H. Moore, "Reflectance-based detection of oxidizers in ambient air," *Sens. Actuator B-Chem.* **227**, 399-402 (2016).

3. A.P. Malanoski; B.J. Johnson; J.S. Erickson; D.A. Stenger, "Development of a Detection Algorithm for Use with Reflectance-Based, Real-Time Chemical Sensing," *Sensors* **16**, 1927 (2016).
4. B.J. Johnson; A.P. Malanoski; J.S. Erickson; R. Liu; A.R. Remenapp; D.A. Stenger; M.H. Moore, "Reflectance-based detection for long term environmental monitoring," *Heliyon* **3**, e00312 (2017).
5. K.A. Connors *Binding Constants: The Measurement of Molecular Complex Stability*; John Wiley & Sons: New York, 1987.
6. K. Linnet; M. Kondratovich, "Partly nonparametric approach for determining the limit of detection," *Clin. Chem.* **50**, 732-740 (2004).

Appendix A

ABSORBANCE DATA

Figure A-1. Absorbance spectra (top) of N_4TPP (9.86 μM) in the absence and presence of increasing concentrations of ethanol: 57, 113, 169, 225, 280, 335, 390, and 444 mM. Arrows indicate increasing target concentration. Absorbance spectra have been corrected for dilution resulting from target addition. Difference absorbance spectra (bottom) are calculated as porphyrin + target <u>minus</u> porphyrin. The concentration dependence of features in the absorbance spectra is also presented (right). Here, the change in absorbance at the trough positions (456 and 730 nm) is plotted against target concentration.

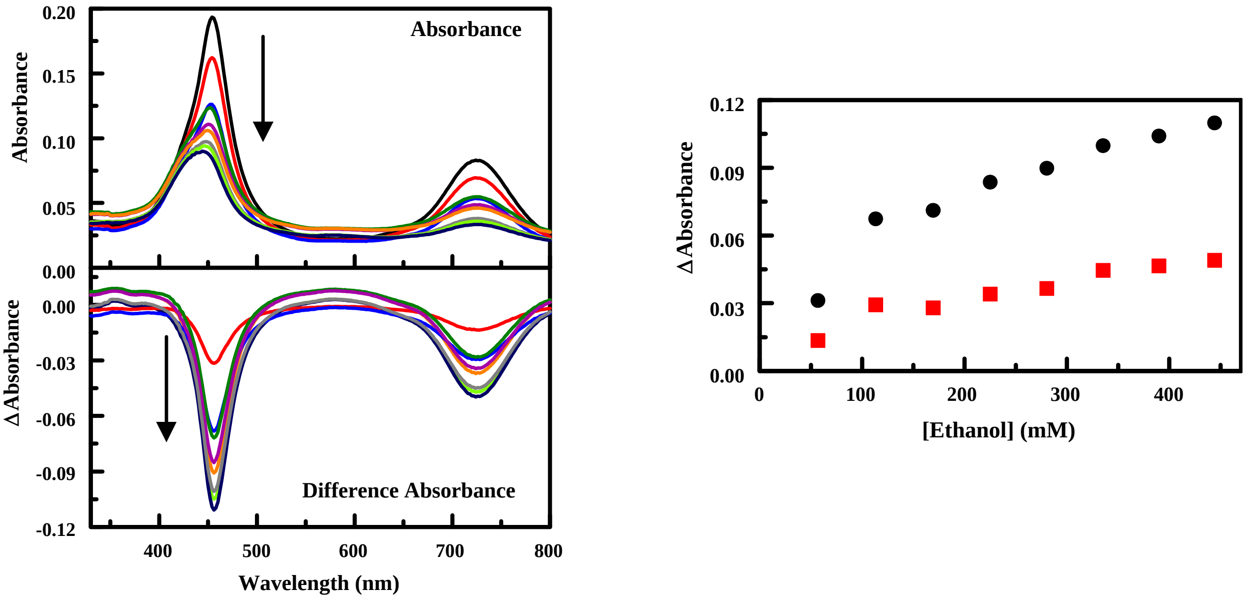

Figure A-2. Absorbance spectra (top) of N_4TPP (9.86 μM) in the absence and presence of increasing concentrations of isopropanol: 43, 86, 129, 171, 214, 256, 298, and 339 mM. Arrows indicate increasing target concentration. Absorbance spectra have been corrected for dilution resulting from target addition. Difference absorbance spectra (bottom) are calculated as porphyrin + target <u>minus</u> porphyrin. The concentration dependence of features in the absorbance spectra is also presented (right). Here, the change in absorbance at the trough positions (456 and 726 nm) is plotted against target concentration.

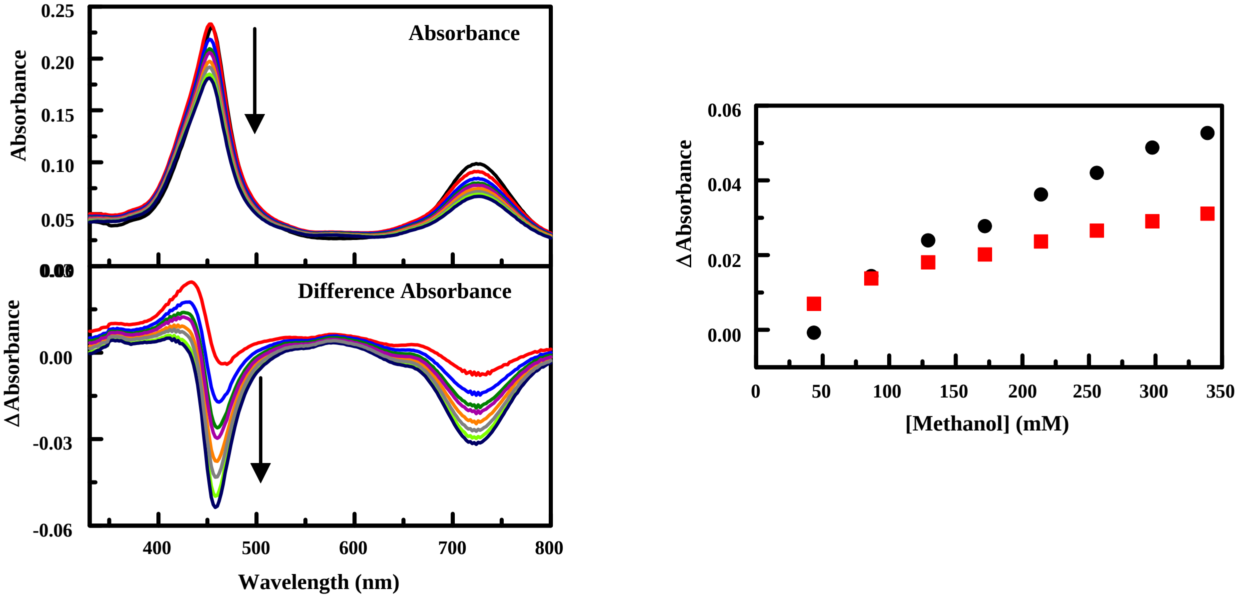

Figure A-3. Absorbance spectra (top) of N_4TPP (9.86 μM) in the absence and presence of increasing concentrations of methanol: 82, 163, 244, 325, 404, 483, 563, and 641 mM. Arrows indicate increasing target concentration. Absorbance spectra have been corrected for dilution resulting from target addition. Difference absorbance spectra (bottom) are calculated as porphyrin + target minus porphyrin. The concentration dependence of features in the absorbance spectra is also presented (right). Here, the change in absorbance at the trough positions (458 and 724 nm) is plotted against target concentration.

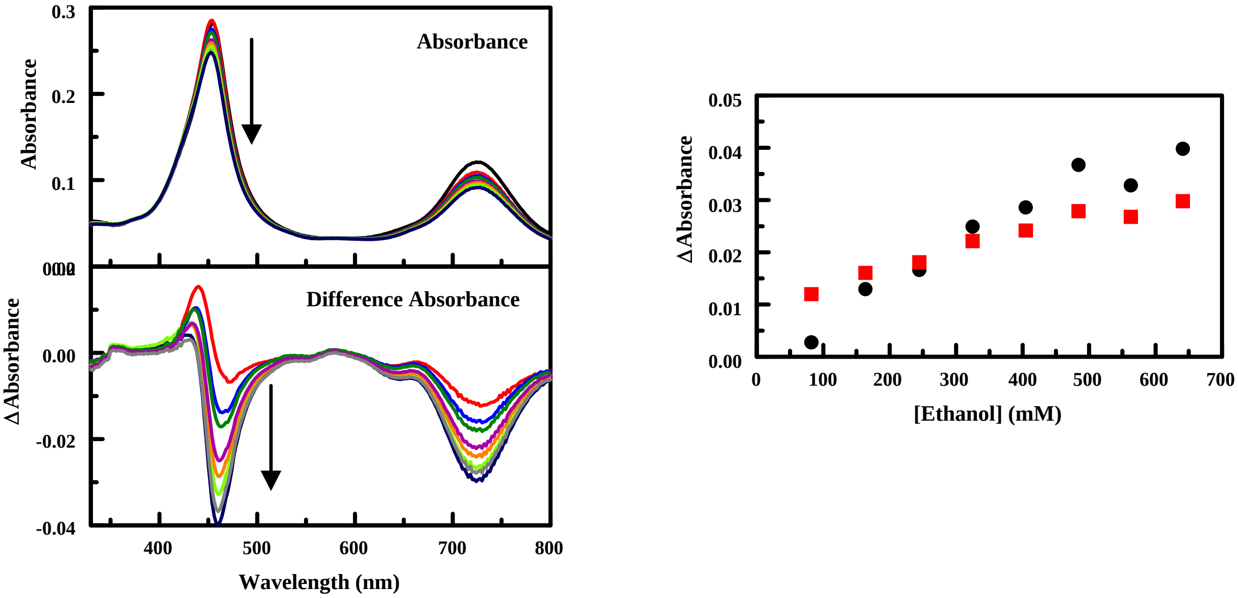

Figure A-4. Absorbance spectra (top) of AgN_4TPP (9.86 μM) in the absence and presence of increasing concentrations of ethanol: 57, 113, 169, 225, 280, 335, 390, and 444 mM. Arrows indicate increasing target concentration. Absorbance spectra have been corrected for dilution resulting from target addition. Difference absorbance spectra (bottom) are calculated as porphyrin + target minus porphyrin. The concentration dependence of features in the absorbance spectra is also presented (right). Here, the change in absorbance at the peak positions (456 and 730 nm) is plotted against target concentration.

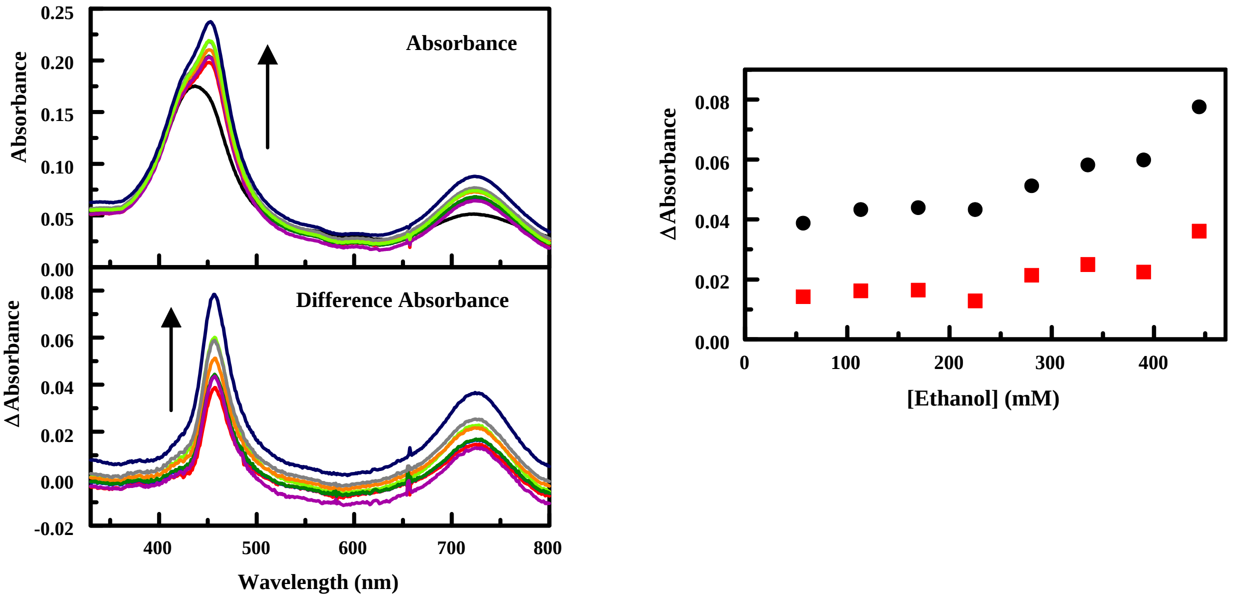

Figure A-5. Absorbance spectra (top) of AgN$_4$TPP (9.86 µM) in the absence and presence of increasing concentrations of isopropanol: 43, 86, 129, 171, 214, 256, 298, and 339 mM. Arrows indicate increasing target concentration. Absorbance spectra have been corrected for dilution resulting from target addition. Difference absorbance spectra (bottom) are calculated as porphyrin + target <u>minus</u> porphyrin. The concentration dependence of features in the absorbance spectra is also presented (right). Here, the change in absorbance at the trough positions (453 and 402 nm) is plotted against target concentration.

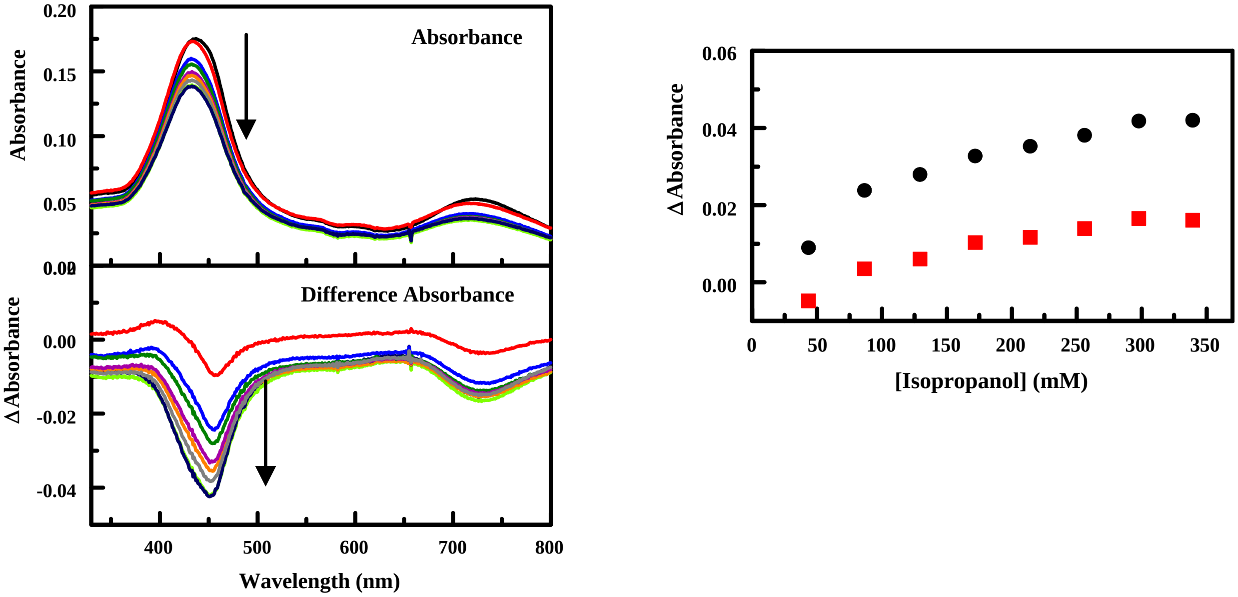

Figure A-6. Absorbance spectra (top) of AgN$_4$TPP (9.86 µM) in the absence and presence of increasing concentrations of methanol: 82, 163, 244, 325, 404, 483, 563, and 641 mM. Arrows indicate increasing target concentration. Absorbance spectra have been corrected for dilution resulting from target addition. Difference absorbance spectra (bottom) are calculated as porphyrin + target <u>minus</u> porphyrin. The concentration dependence of features in the absorbance spectra is also presented (right). Here, the change in absorbance at the trough positions (458 and 714 nm) is plotted against target concentration.

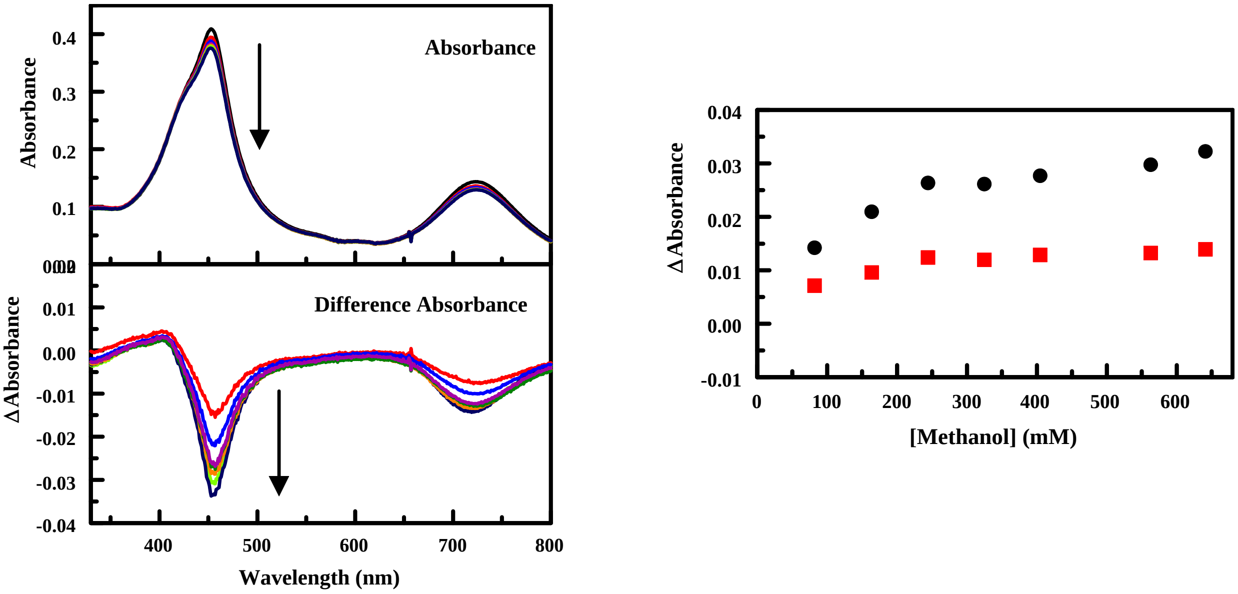

Figure A-7. Absorbance spectra (top) of CdN$_4$TPP (9.86 μM) in the absence and presence of increasing concentrations of ethanol: 57, 113, 169, 225, 280, 335, 390, and 444 mM. Arrows indicate increasing target concentration. Absorbance spectra have been corrected for dilution resulting from target addition. Difference absorbance spectra (bottom) are calculated as porphyrin + target minus porphyrin. The concentration dependence of features in the absorbance spectra is also presented (right). Here, the change in absorbance at the trough positions (456 and 727 nm) is plotted against target concentration.

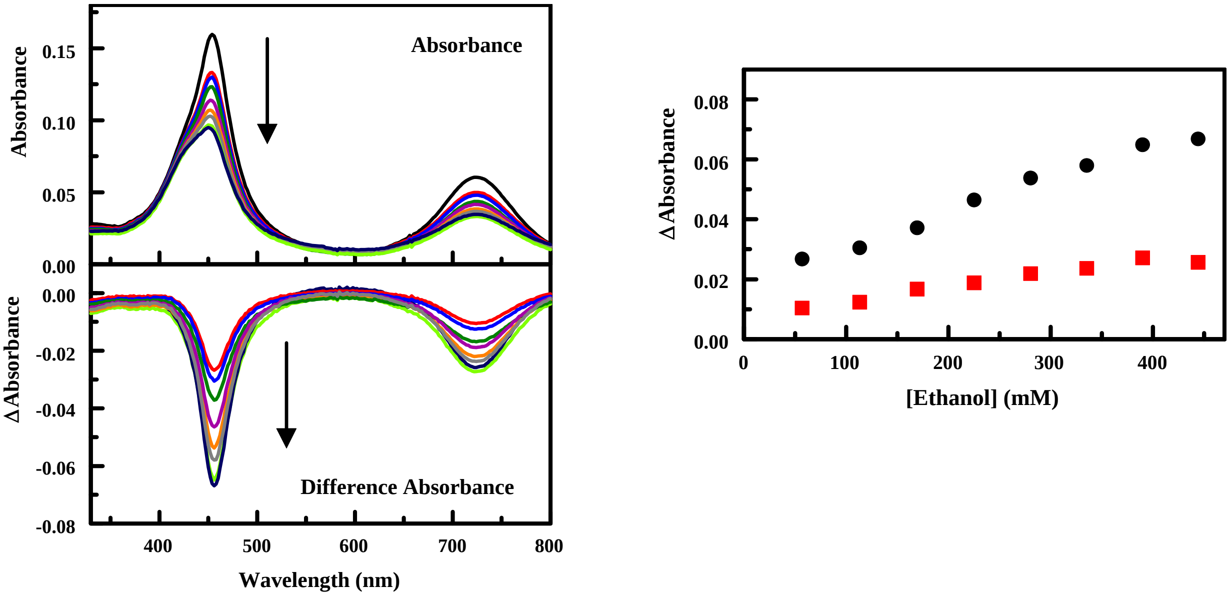

Figure A-8. Absorbance spectra (top) of CdN$_4$TPP (9.86 μM) in the absence and presence of increasing concentrations of isopropanol: 43, 86, 129, 171, 214, 256, 298, and 339 mM. Arrows indicate increasing target concentration. Absorbance spectra have been corrected for dilution resulting from target addition. Difference absorbance spectra (bottom) are calculated as porphyrin + target minus porphyrin. The concentration dependence of features in the absorbance spectra is also presented (right). Here, the change in absorbance at the trough positions (458 and 582 nm) is plotted against target concentration.

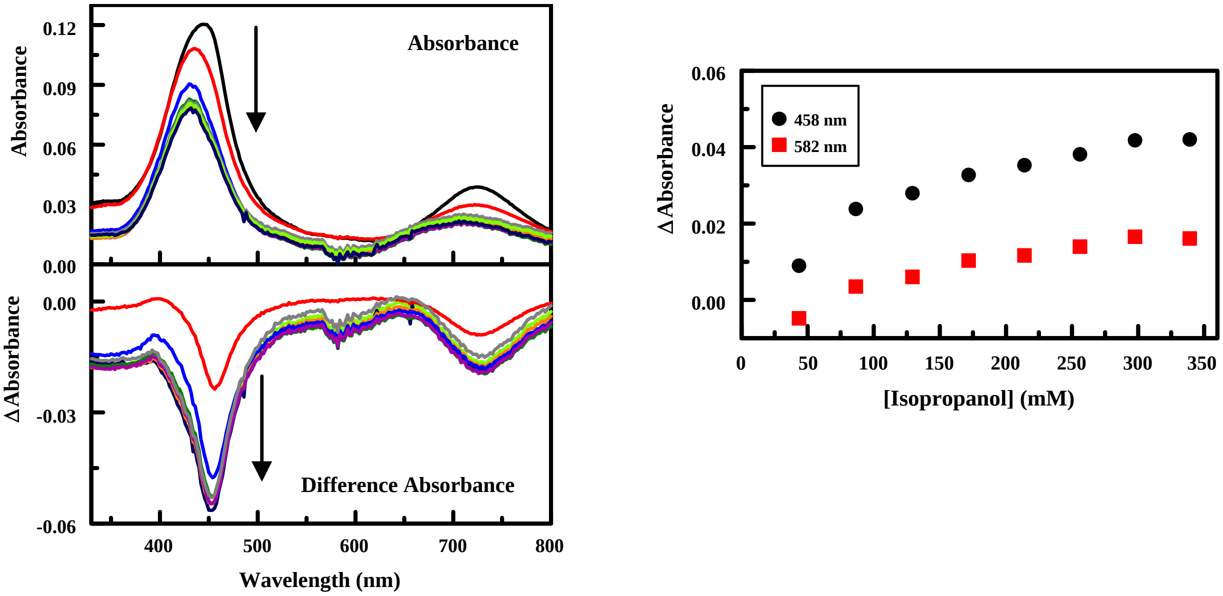

Figure A-9. Absorbance spectra (top) of CdN$_4$TPP (9.86 μM) in the absence and presence of increasing concentrations of methanol: 82, 163, 244, 325, 404, 483, 563, and 641 mM. Arrows indicate increasing target concentration. Absorbance spectra have been corrected for dilution resulting from target addition. Difference absorbance spectra (bottom) are calculated as porphyrin + target minus porphyrin. The concentration dependence of features in the absorbance spectra is also presented (right). Here, the change in absorbance at the trough positions (458 and 714 nm) is plotted against target concentration.

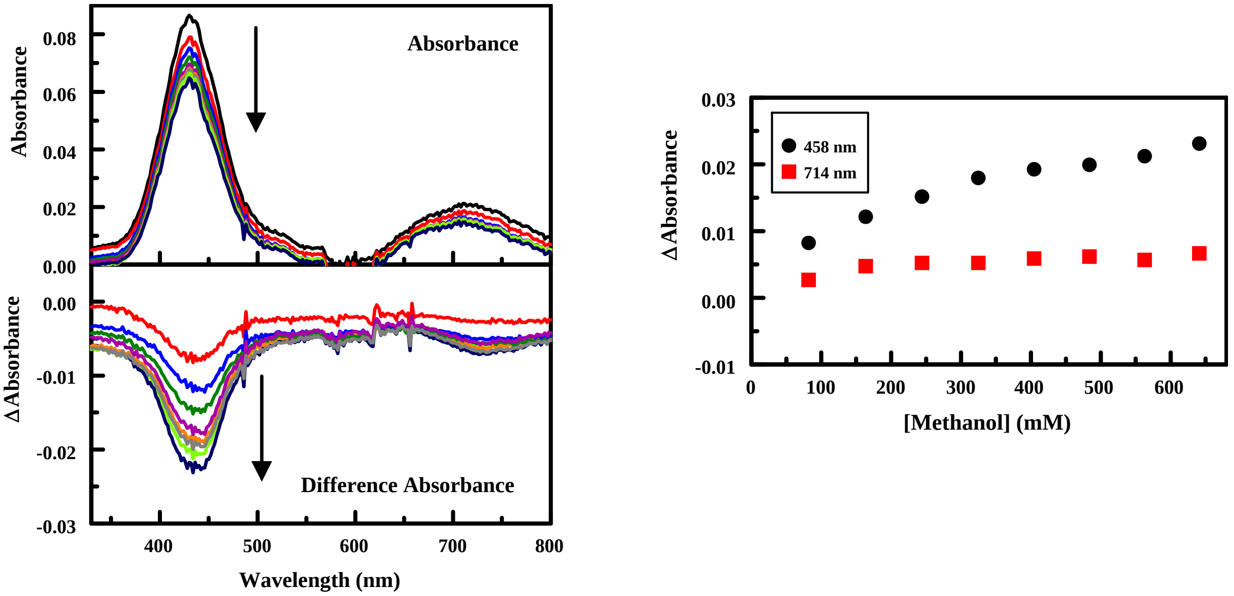

Figure A-10. Absorbance spectra (top) of CeN$_4$TPP (9.86 μM) in the absence and presence of increasing concentrations of ethanol: 57, 113, 169, 225, 280, 335, 390, and 444 mM. Arrows indicate increasing target concentration. Absorbance spectra have been corrected for dilution resulting from target addition. Difference absorbance spectra (bottom) are calculated as porphyrin + target minus porphyrin. The concentration dependence of features in the absorbance spectra is also presented (right). Here, the change in absorbance at the trough positions (466 and 728 nm) is plotted against target concentration.

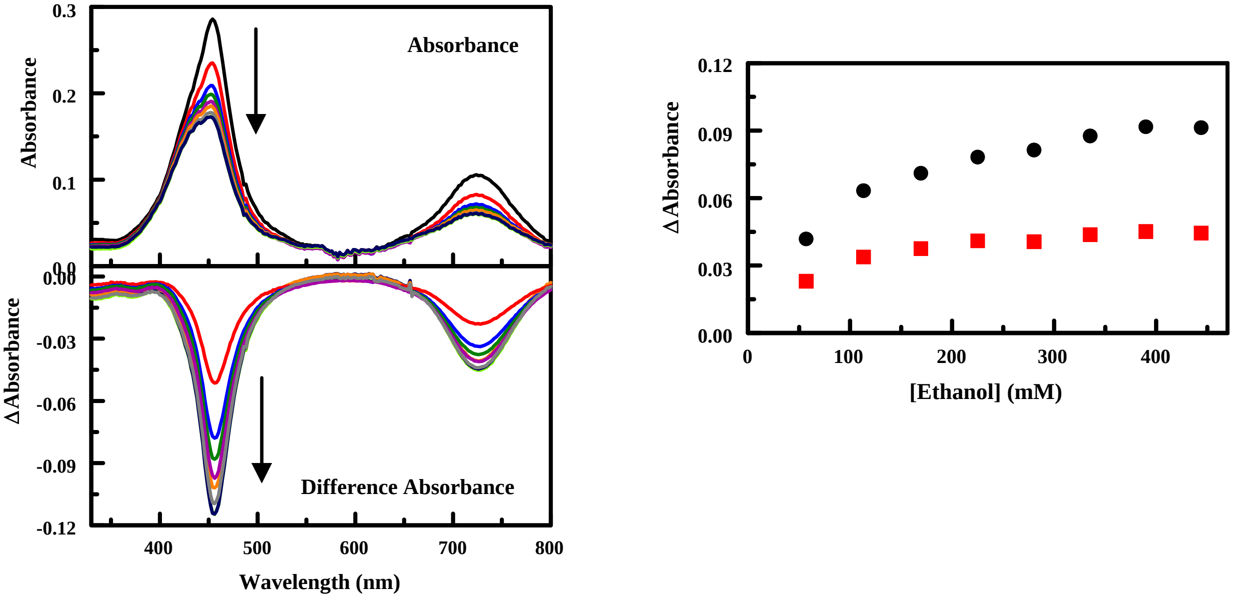

Figure A-11. Absorbance spectra (top) of CeN$_4$TPP (9.86 μM) in the absence and presence of increasing concentrations of isopropanol: 43, 86, 129, 171, 214, 256, 298, and 339 mM. Arrows indicate increasing target concentration. Absorbance spectra have been corrected for dilution resulting from target addition. Difference absorbance spectra (bottom) are calculated as porphyrin + target minus porphyrin. The concentration dependence of features in the absorbance spectra is also presented (right). Here, the change in absorbance at the trough positions (454 and 732 nm) is plotted against target concentration.

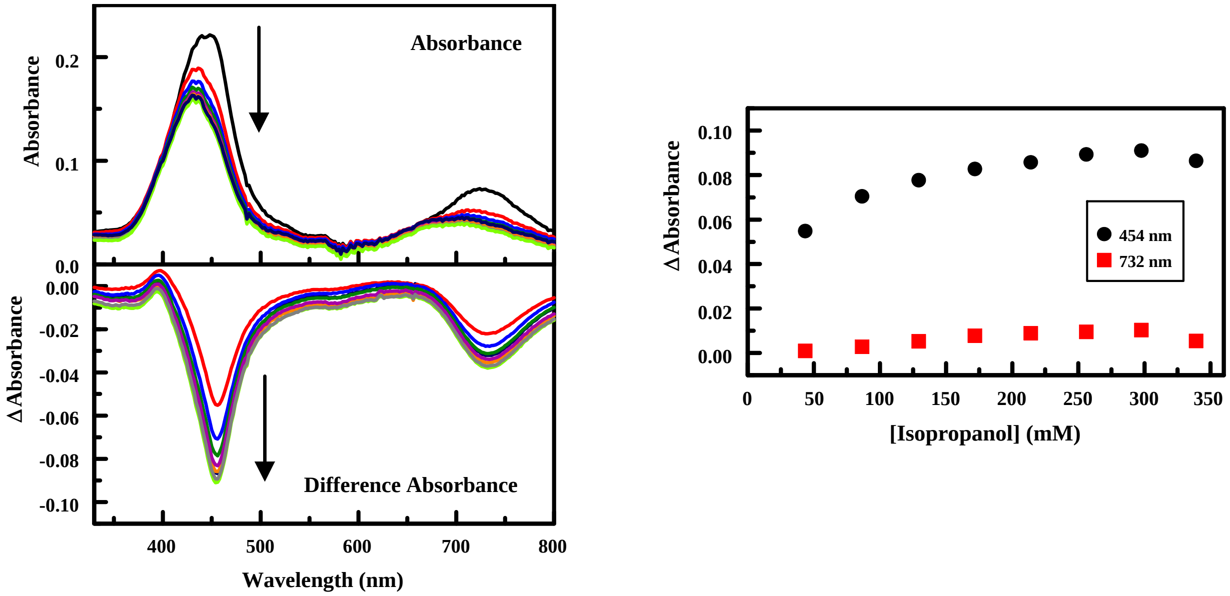

Figure A-12. Absorbance spectra (top) of CeN$_4$TPP (9.86 μM) in the absence and presence of increasing concentrations of methanol: 82, 163, 244, 325, 404, 483, 563, and 641 mM. Arrows indicate increasing target concentration. Absorbance spectra have been corrected for dilution resulting from target addition. Difference absorbance spectra (bottom) are calculated as porphyrin + target minus porphyrin. The concentration dependence of features in the absorbance spectra is also presented (right). Here, the change in absorbance at the trough positions (458 and 730 nm) is plotted against target concentration.

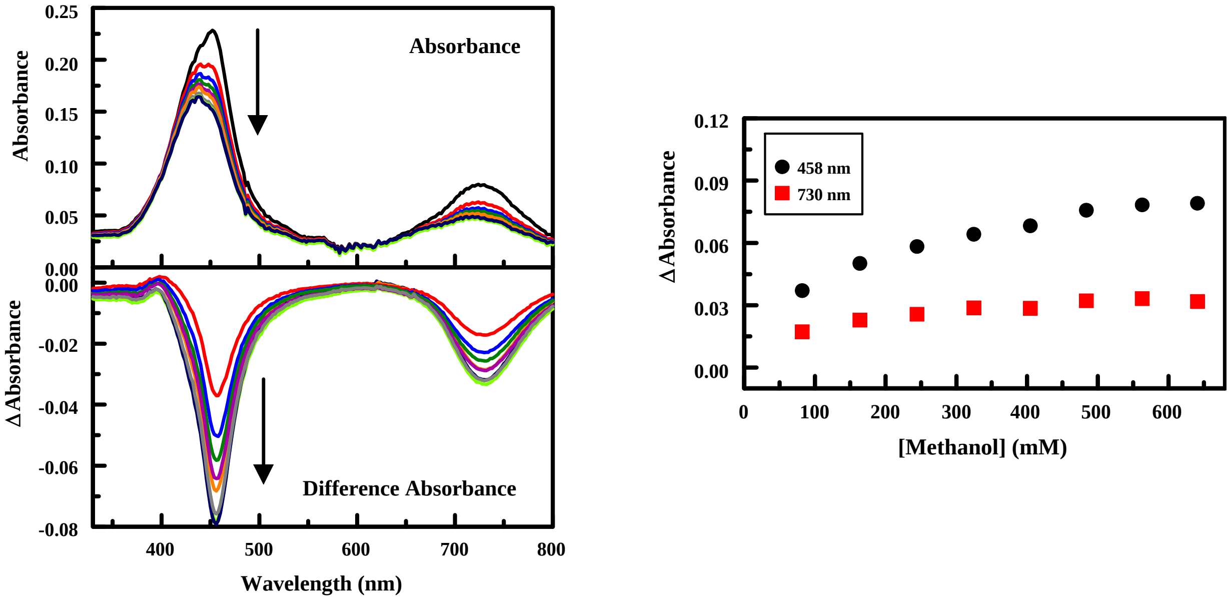

Figure A-13. Absorbance spectra (top) of CoN$_4$TPP (9.86 µM) in the absence and presence of increasing concentrations of ethanol: 57, 113, 169, 225, 280, 335, 390, and 444 mM. Arrows indicate increasing target concentration. Absorbance spectra have been corrected for dilution resulting from target addition. Difference absorbance spectra (bottom) are calculated as porphyrin + target <u>minus</u> porphyrin. The concentration dependence of features in the absorbance spectra is also presented (right). Here, the change in absorbance at the trough positions (442 and 578 nm) is plotted against target concentration.

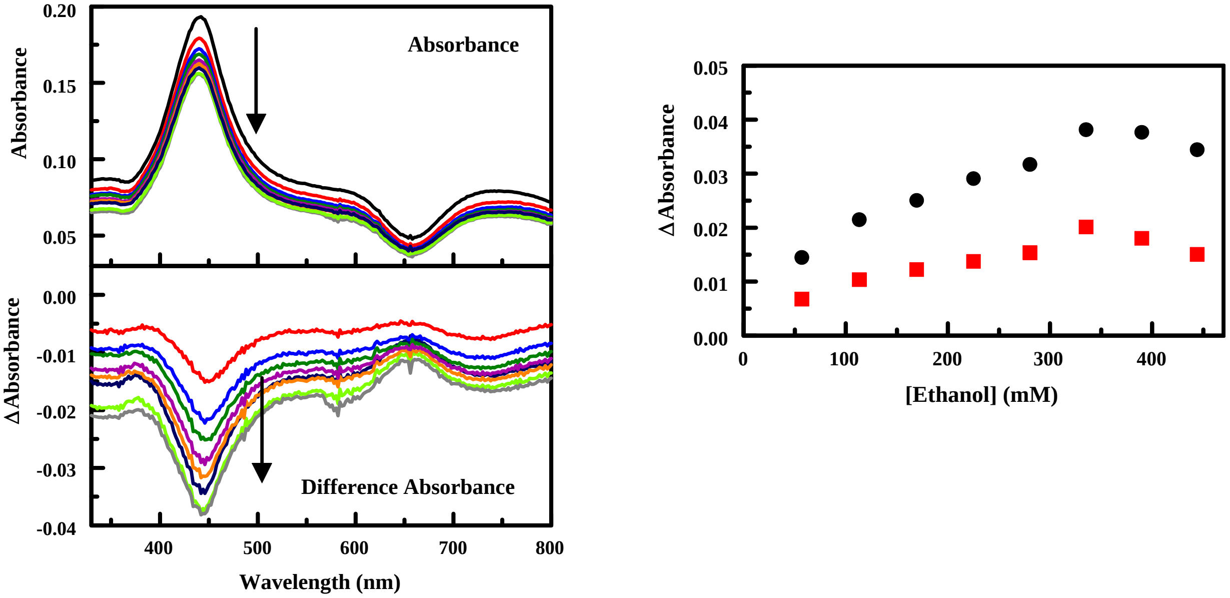

Figure A-14. Absorbance spectra (top) of CoN$_4$TPP (9.86 µM) in the absence and presence of increasing concentrations of isopropanol: 43, 86, 129, 171, 214, 256, 298, and 339 mM. Arrows indicate increasing target concentration. Absorbance spectra have been corrected for dilution resulting from target addition. Difference absorbance spectra (bottom) are calculated as porphyrin + target <u>minus</u> porphyrin. The concentration dependence of features in the absorbance spectra is also presented (right). Here, the change in absorbance at the trough positions (442 and 570 nm) is plotted against target concentration.

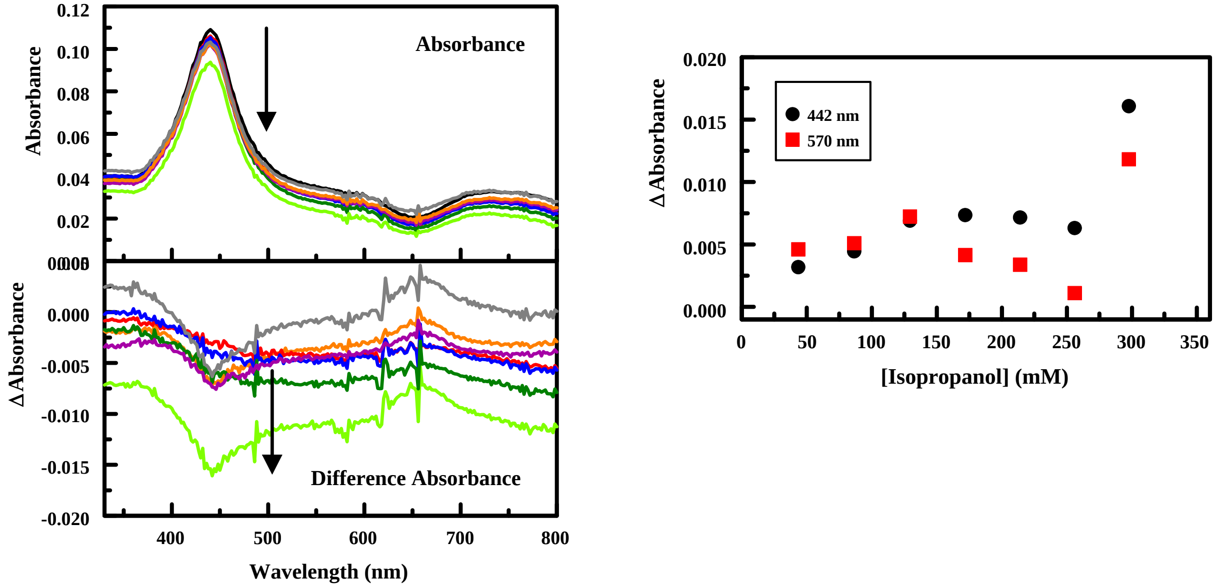

Figure A-15. Absorbance spectra (top) of CoN$_4$TPP (9.86 μM) in the absence and presence of increasing concentrations of methanol: 82, 163, 244, 325, 404, 483, 563, and 641 mM. Arrows indicate increasing target concentration. Absorbance spectra have been corrected for dilution resulting from target addition. Difference absorbance spectra (bottom) are calculated as porphyrin + target <u>minus</u> porphyrin. The concentration dependence of features in the absorbance spectra is also presented (right). Here, the change in absorbance at the trough positions (458 and 730 nm) is plotted against target concentration.

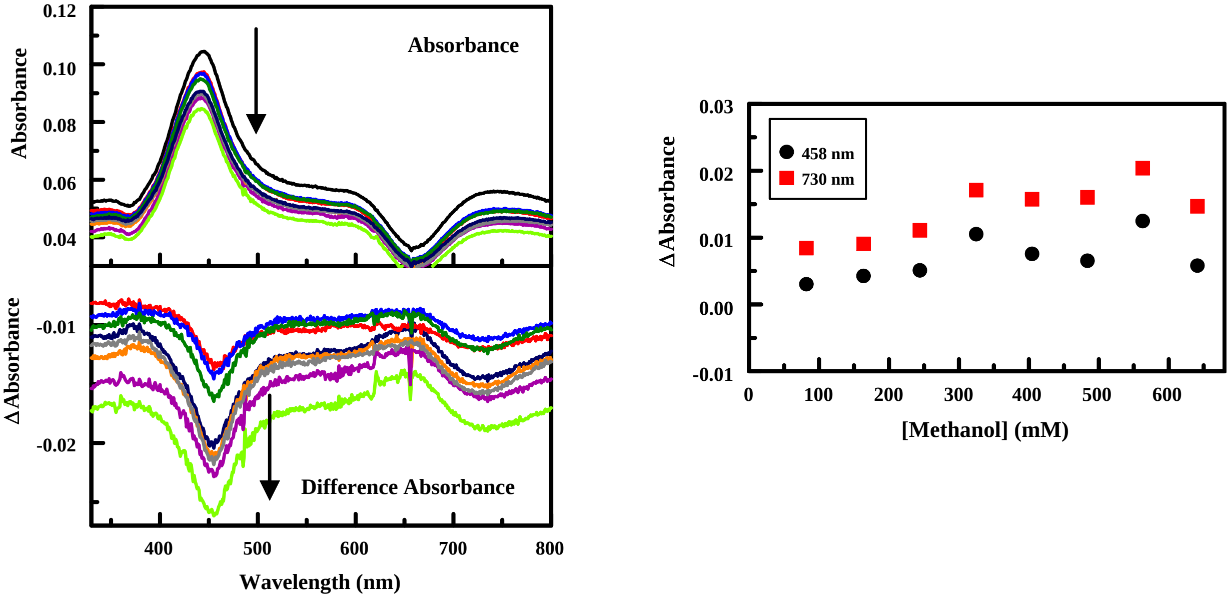

Figure A-16. Absorbance spectra (top) of CuN$_4$TPP (9.86 μM) in the absence and presence of increasing concentrations of ethanol: 57, 113, 169, 225, 280, 335, 390, and 444 mM. Arrows indicate increasing target concentration. Absorbance spectra have been corrected for dilution resulting from target addition. Difference absorbance spectra (bottom) are calculated as porphyrin + target <u>minus</u> porphyrin. The concentration dependence of features in the absorbance spectra is also presented (right). Here, the change in absorbance at the trough positions (411 and 452 nm) is plotted against target concentration.

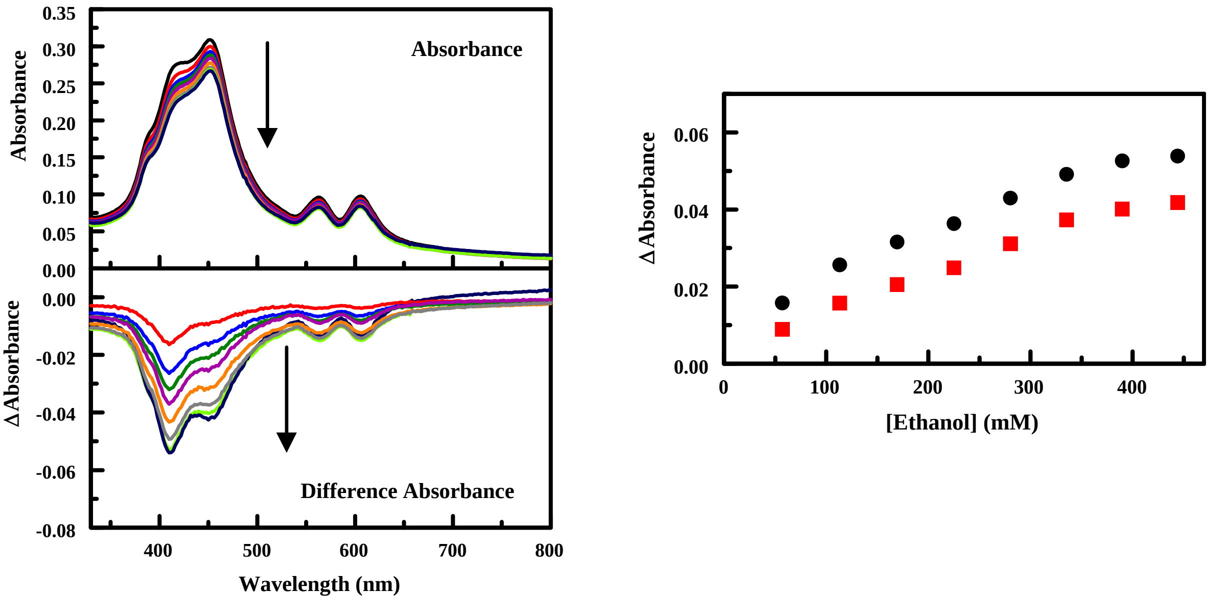

Figure A-17. Absorbance spectra (top) of CuN_4TPP (9.86 μM) in the absence and presence of increasing concentrations of isopropanol: 43, 86, 129, 171, 214, 256, 298, and 339 mM. Arrows indicate increasing target concentration. Absorbance spectra have been corrected for dilution resulting from target addition. Difference absorbance spectra (bottom) are calculated as porphyrin + target minus porphyrin. The concentration dependence of features in the absorbance spectra is also presented (right). Here, the change in absorbance at the trough positions (416 and 454 nm) is plotted against target concentration.

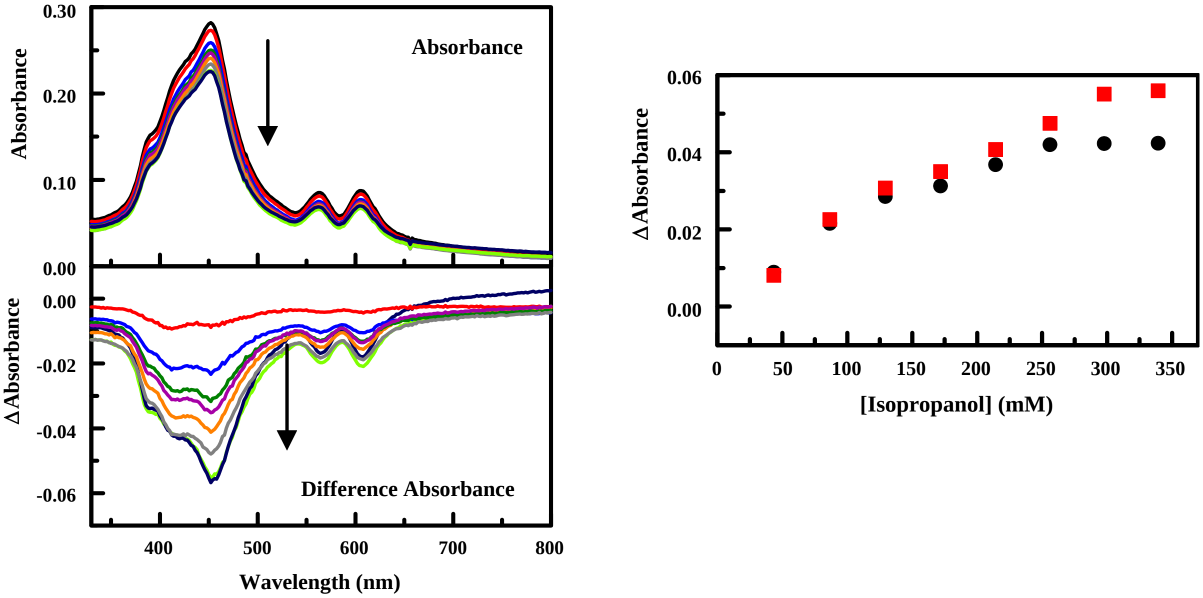

Figure A-18. Absorbance spectra (top) of CuN_4TPP (9.86 μM) in the absence and presence of increasing concentrations of methanol: 82, 163, 244, 325, 404, 483, 563, and 641 mM. Arrows indicate increasing target concentration. Absorbance spectra have been corrected for dilution resulting from target addition. Difference absorbance spectra (bottom) are calculated as porphyrin + target minus porphyrin. The concentration dependence of features in the absorbance spectra is also presented (right). Here, the change in absorbance at the trough positions (411 and 452 nm) is plotted against target concentration.

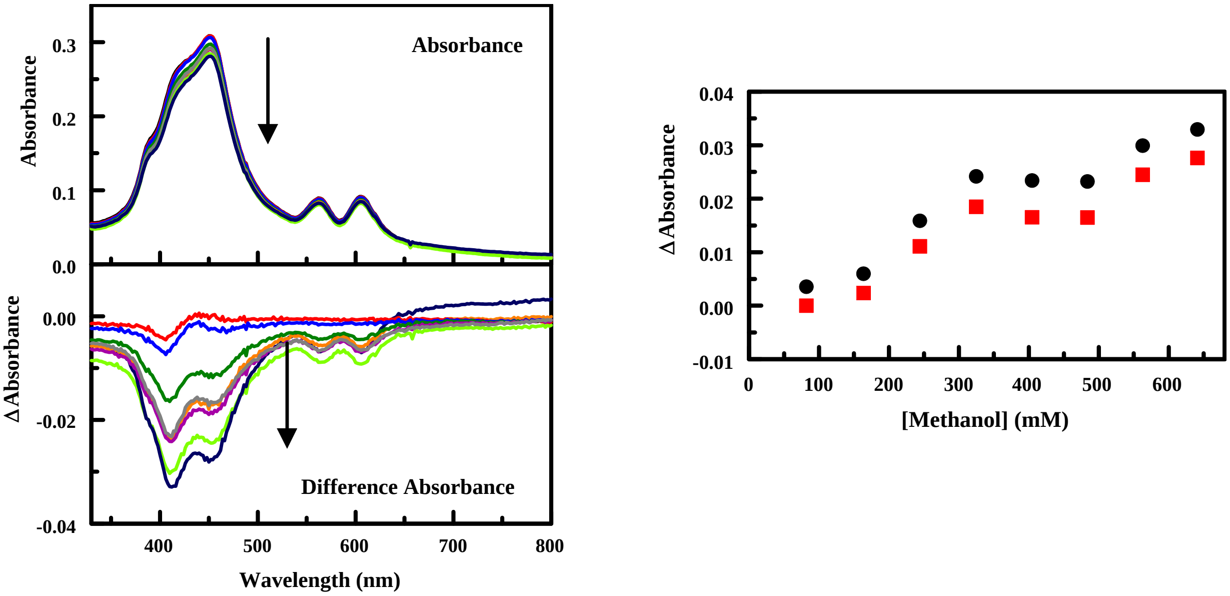

Figure A-19. Absorbance spectra (top) of FeN$_4$TPP (9.86 μM) in the absence and presence of increasing concentrations of ethanol: 57, 113, 169, 225, 280, 335, 390, and 444 mM. Arrows indicate increasing target concentration. Absorbance spectra have been corrected for dilution resulting from target addition. Difference absorbance spectra (bottom) are calculated as porphyrin + target <u>minus</u> porphyrin. The concentration dependence of features in the absorbance spectra is also presented (right). Here, the change in absorbance at the peak positions (454 and 730 nm) is plotted against target concentration.

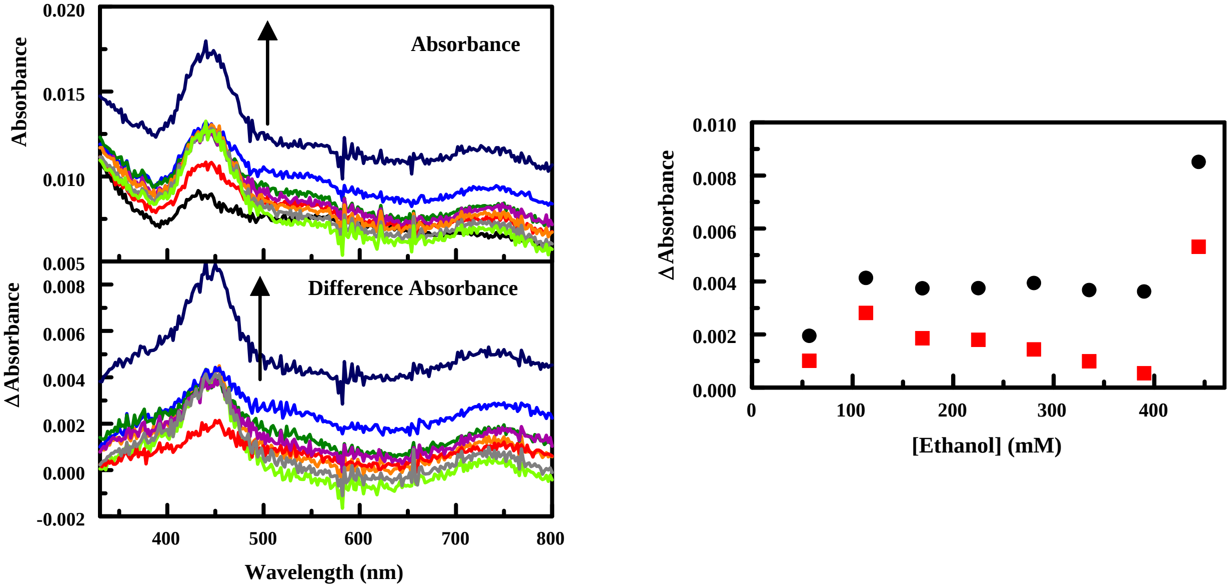

Figure A-20. Absorbance spectra (top) of FeN$_4$TPP (9.86 μM) in the absence and presence of increasing concentrations of isopropanol: 43, 86, 129, 171, 214, 256, 298, and 339 mM. Arrows indicate increasing target concentration. Absorbance spectra have been corrected for dilution resulting from target addition. Difference absorbance spectra (bottom) are calculated as porphyrin + target <u>minus</u> porphyrin. The concentration dependence of features in the absorbance spectra is also presented (right). Here, the change in absorbance at the peak positions (454 and 730 nm) is plotted against target concentration.

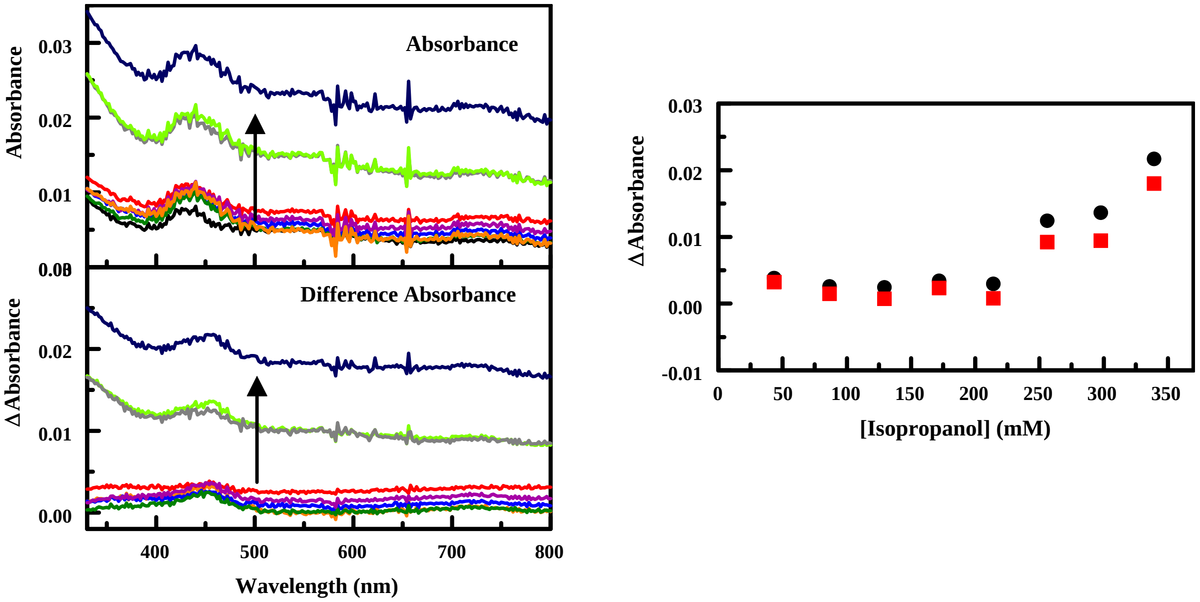

Figure A-21. Absorbance spectra (top) of FeN$_4$TPP (9.86 μM) in the absence and presence of increasing concentrations of methanol: 82, 163, 244, 325, 404, 483, 563, and 641 mM. Arrows indicate increasing target concentration. Absorbance spectra have been corrected for dilution resulting from target addition. Difference absorbance spectra (bottom) are calculated as porphyrin + target minus porphyrin. The concentration dependence of features in the absorbance spectra is also presented (right). Here, the change in absorbance at the peak positions (411 and 452 nm) is plotted against target concentration.

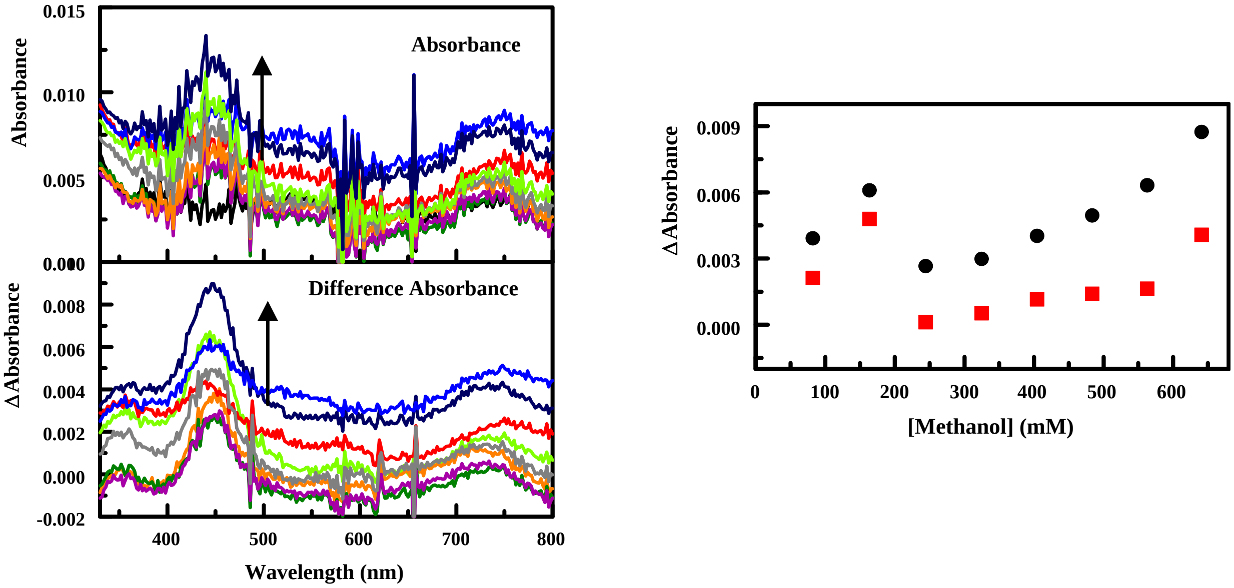

Figure A-22. Absorbance spectra (top) of NiN$_4$TPP (9.86 μM) in the absence and presence of increasing concentrations of ethanol: 57, 113, 169, 225, 280, 335, 390, and 444 mM. Arrows indicate increasing target concentration. Absorbance spectra have been corrected for dilution resulting from target addition. Difference absorbance spectra (bottom) are calculated as porphyrin + target minus porphyrin. The concentration dependence of features in the absorbance spectra is also presented (right). Here, the change in absorbance at the trough positions (454 and 730 nm) is plotted against target concentration.

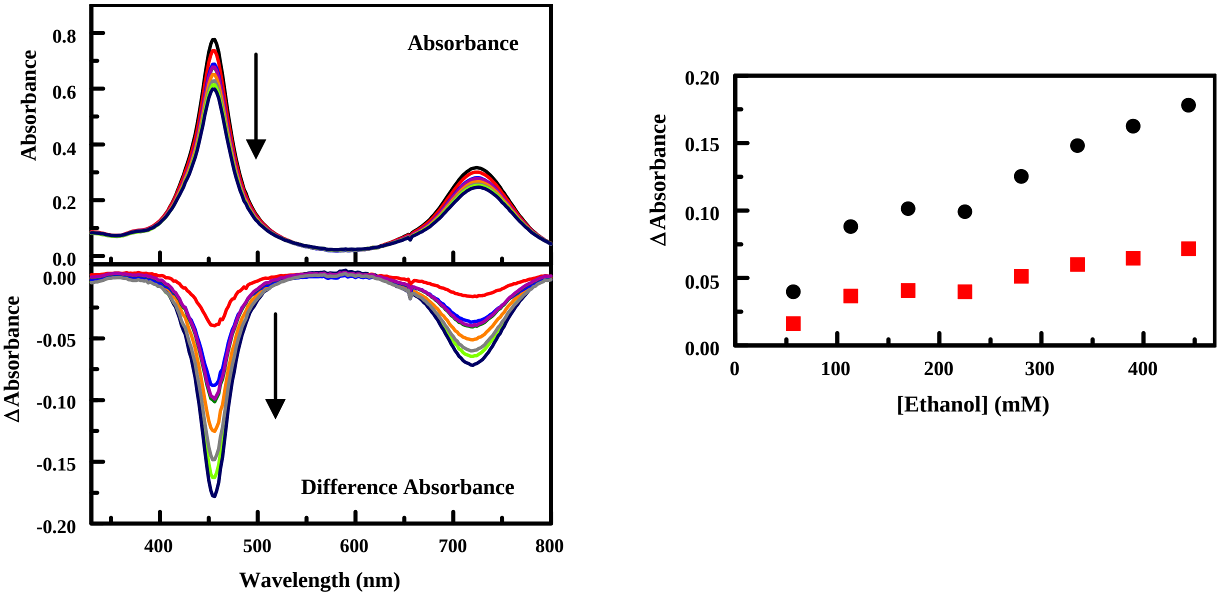

Figure A-23. Absorbance spectra (top) of NiN_4TPP (9.86 μM) in the absence and presence of increasing concentrations of isopropanol: 43, 86, 129, 171, 214, 256, 298, and 339 mM. Arrows indicate increasing target concentration. Absorbance spectra have been corrected for dilution resulting from target addition. Difference absorbance spectra (bottom) are calculated as porphyrin + target minus porphyrin. The concentration dependence of features in the absorbance spectra is also presented (right). Here, the change in absorbance at the trough positions (454 and 730 nm) is plotted against target concentration.

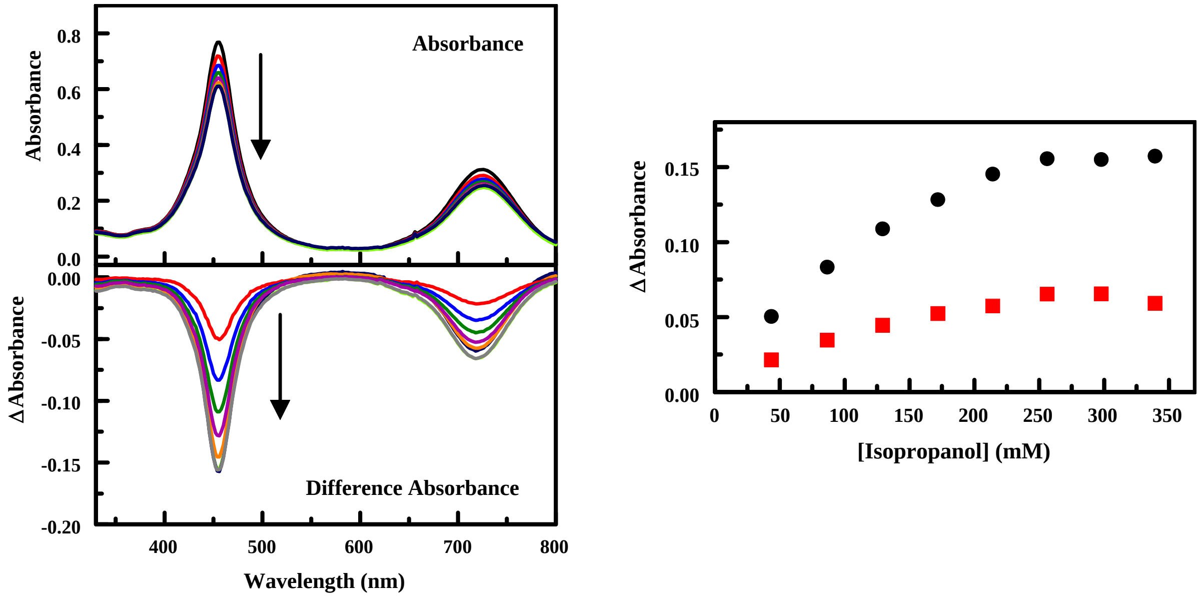

Figure A-24. Absorbance spectra (top) of NiN_4TPP (9.86 μM) in the absence and presence of increasing concentrations of methanol: 82, 163, 244, 325, 404, 483, 563, and 641 mM. Arrows indicate increasing target concentration. Absorbance spectra have been corrected for dilution resulting from target addition. Difference absorbance spectra (bottom) are calculated as porphyrin + target minus porphyrin. The concentration dependence of features in the absorbance spectra is also presented (right). Here, the change in absorbance at the trough positions (454 and 730 nm) is plotted against target concentration.

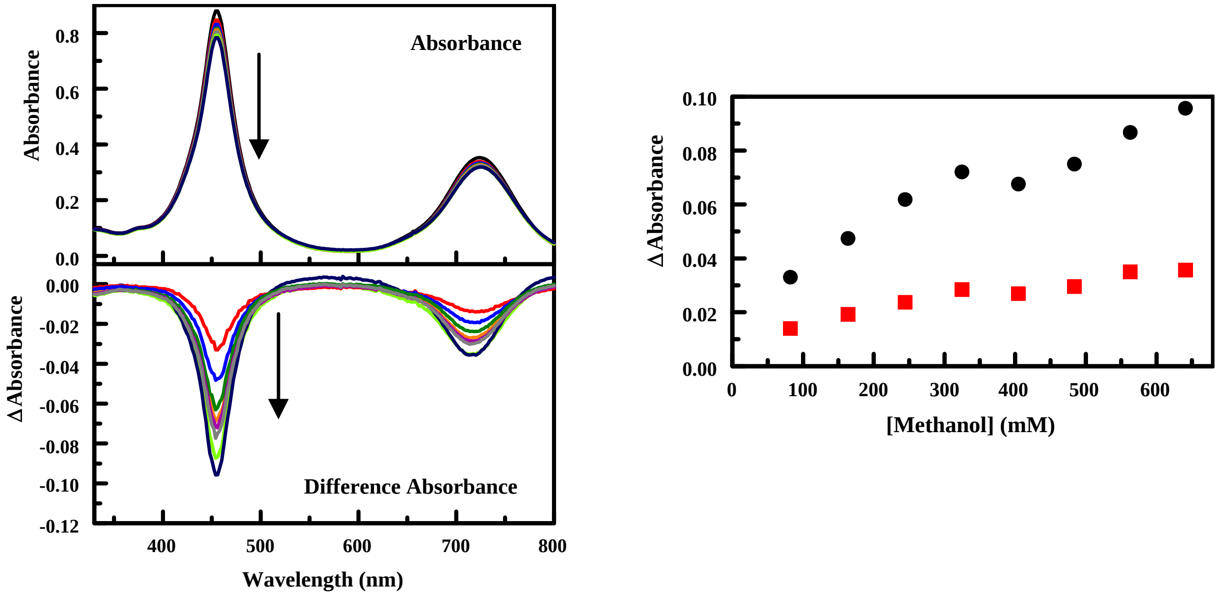

Figure A-25. Absorbance spectra (top) of YN$_4$TPP (9.86 µM) in the absence and presence of increasing concentrations of ethanol: 57, 113, 169, 225, 280, 335, 390, and 444 mM. Arrows indicate increasing target concentration. Absorbance spectra have been corrected for dilution resulting from target addition. Difference absorbance spectra (bottom) are calculated as porphyrin + target <u>minus</u> porphyrin. The concentration dependence of features in the absorbance spectra is also presented (right). Here, the change in absorbance at the trough positions (456 and 712 nm) is plotted against target concentration.

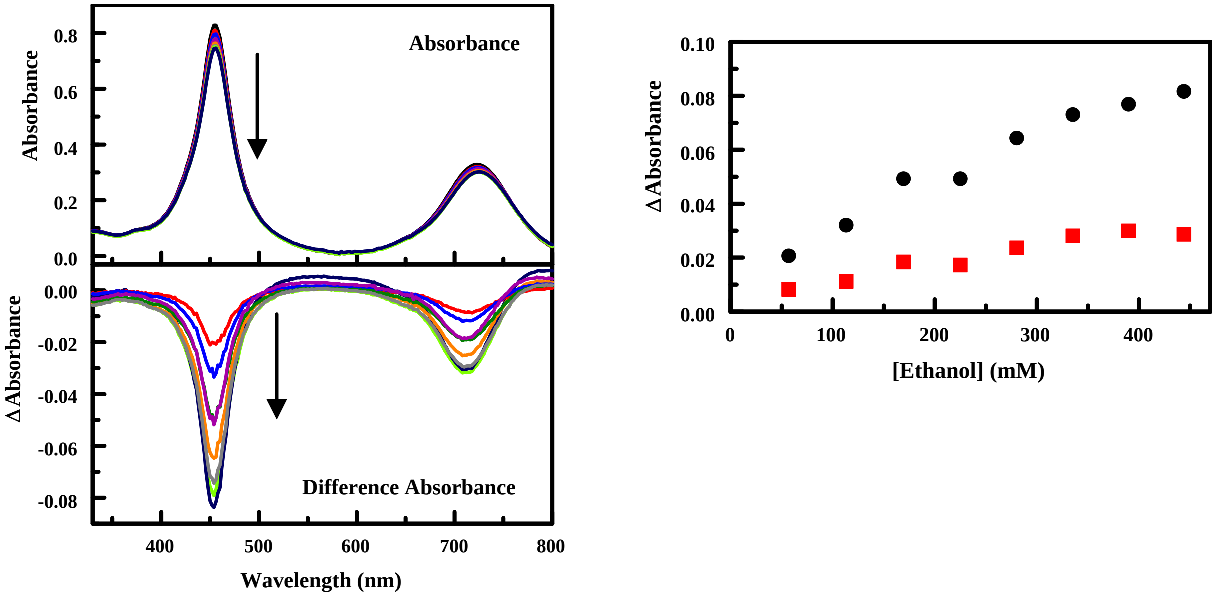

Figure A-26. Absorbance spectra (top) of YN$_4$TPP (9.86 µM) in the absence and presence of increasing concentrations of isopropanol: 43, 86, 129, 171, 214, 256, 298, and 339 mM. Arrows indicate increasing target concentration. Absorbance spectra have been corrected for dilution resulting from target addition. Difference absorbance spectra (bottom) are calculated as porphyrin + target <u>minus</u> porphyrin. The concentration dependence of features in the absorbance spectra is also presented (right). Here, the change in absorbance at the trough positions (456 and 712 nm) is plotted against target concentration.

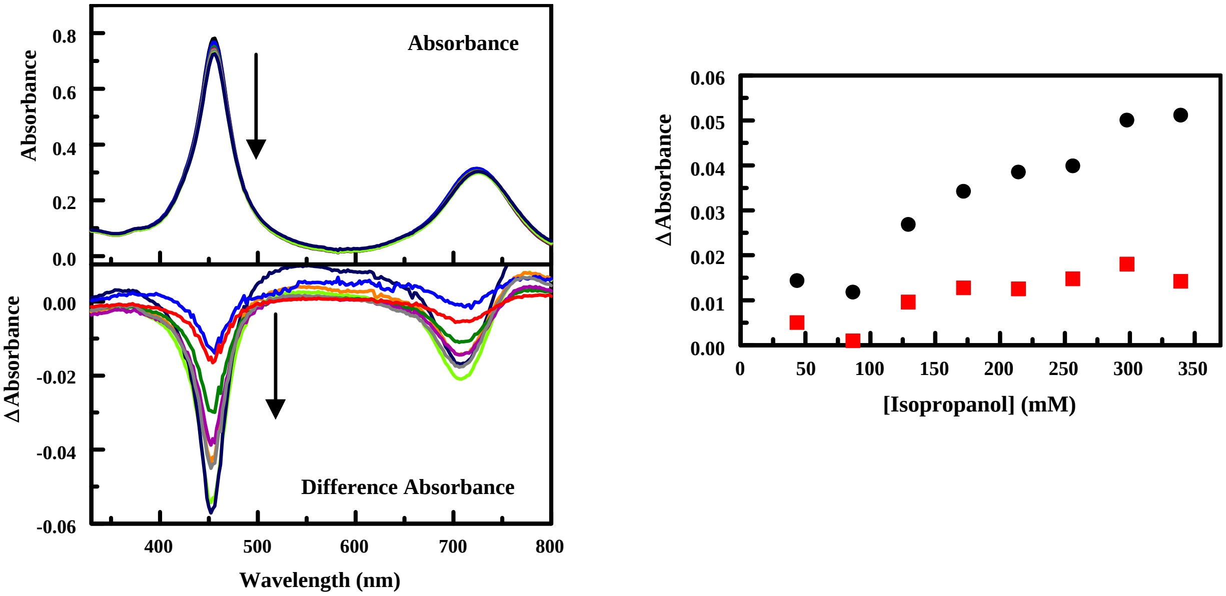

Figure A-27. Absorbance spectra (top) of YN_4TPP (9.86 μM) in the absence and presence of increasing concentrations of methanol: 82, 163, 244, 325, 404, 483, 563, and 641 mM. Arrows indicate increasing target concentration. Absorbance spectra have been corrected for dilution resulting from target addition. Difference absorbance spectra (bottom) are calculated as porphyrin + target <u>minus</u> porphyrin. The concentration dependence of features in the absorbance spectra is also presented (right). Here, the change in absorbance at the trough positions (456 and 712 nm) is plotted against target concentration.

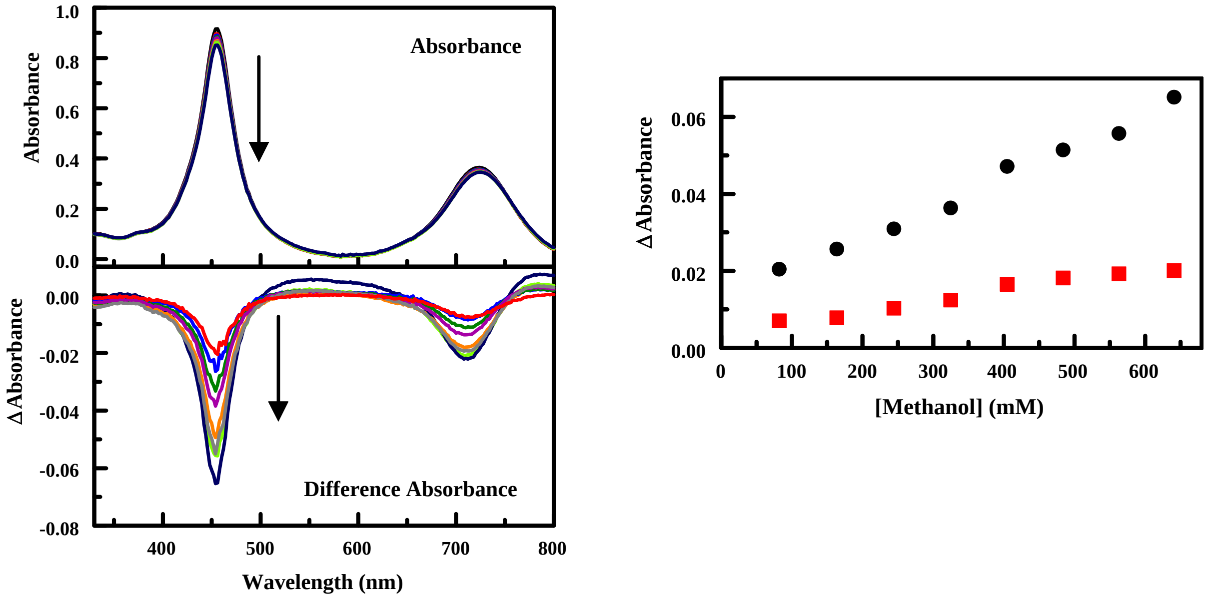

Figure A-28. Absorbance spectra (top) of ZnN_4TPP (9.86 μM) in the absence and presence of increasing concentrations of ethanol: 57, 113, 169, 225, 280, 335, 390, and 444 mM. Arrows indicate increasing target concentration. Absorbance spectra have been corrected for dilution resulting from target addition. Difference absorbance spectra (bottom) are calculated as porphyrin + target <u>minus</u> porphyrin. The concentration dependence of features in the absorbance spectra is also presented (right). Here, the change in absorbance at the trough positions (458 and 720 nm) is plotted against target concentration.

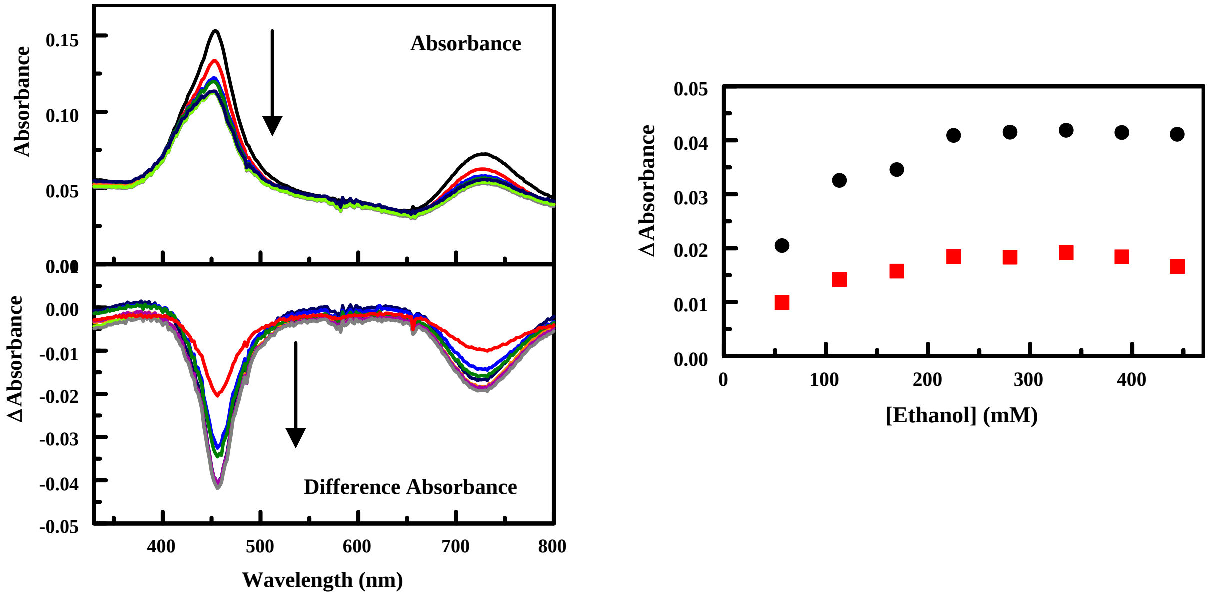

Figure A-29. Absorbance spectra (top) of ZnN_4TPP (9.86 µM) in the absence and presence of increasing concentrations of isopropanol: 43, 86, 129, 171, 214, 256, 298, and 339 mM. Arrows indicate increasing target concentration. Absorbance spectra have been corrected for dilution resulting from target addition. Difference absorbance spectra (bottom) are calculated as porphyrin + target <u>minus</u> porphyrin. The concentration dependence of features in the absorbance spectra is also presented (right). Here, the change in absorbance at the trough positions (458 and 720 nm) is plotted against target concentration.

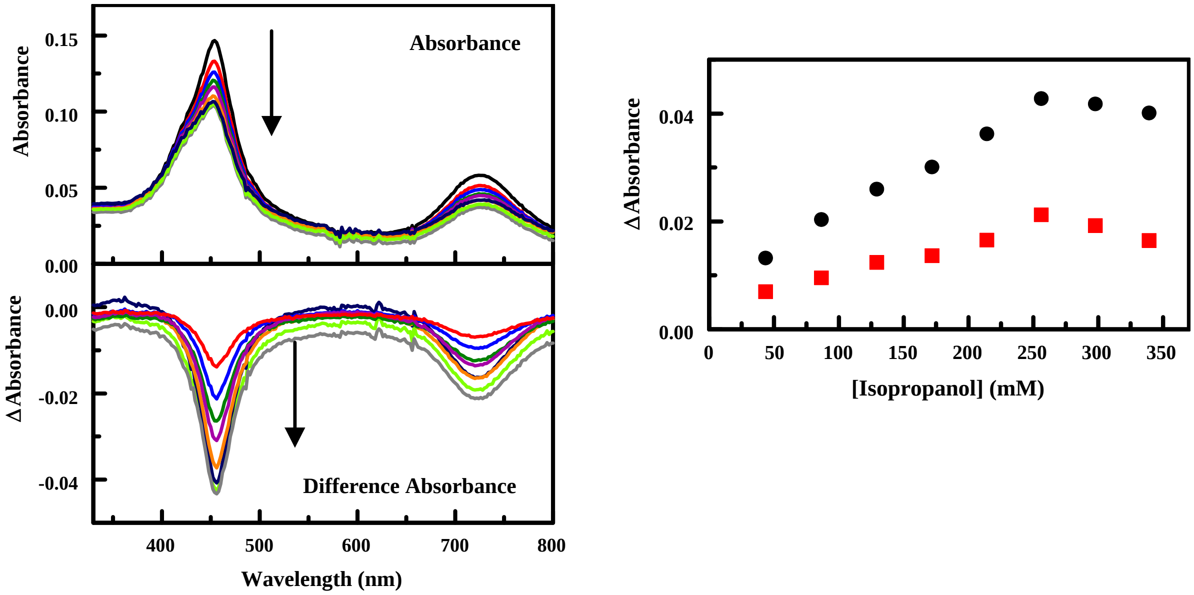

Figure A-30. Absorbance spectra (top) of ZnN_4TPP (9.86 µM) in the absence and presence of increasing concentrations of methanol: 82, 163, 244, 325, 404, 483, 563, and 641 mM. Arrows indicate increasing target concentration. Absorbance spectra have been corrected for dilution resulting from target addition. Difference absorbance spectra (bottom) are calculated as porphyrin + target <u>minus</u> porphyrin. The concentration dependence of features in the absorbance spectra is also presented (right). Here, the change in absorbance at the trough positions (458 and 720 nm) is plotted against target concentration.